J. Fluid Mech. (1991), *vol.* 222, *pp.* 139–155
Printed in Great Britain

Models for high-Reynolds-number flow down a step

By K. O'MALLEY,[1] A. D. FITT,[2] T. V. JONES,[1]
J. R. OCKENDON[3] AND P. WILMOTT[4]

[1] Department of Engineering Science, Parks Rd , Oxford, OX1 3PJ, UK
[2] Mathematics Department, University of Southampton, Hampshire, SO9 5NH, UK
[3] Mathematical Institute, 24–29 St. Giles, Oxford, OX1 3LB, UK
[4] Department of Mathematics, Imperial College of Science & Technology, London, SW7 2BZ, UK

(Received 21 August 1989 and in revised form 26 March 1990)

We consider inviscid, incompressible flow down a backward-facing step. Using thin-aerofoil theory, a model is proposed in which the separated region downstream of the back face of the step consists of a constant-pressure zone immediately behind the step, followed by a Prandtl–Batchelor constant-vorticity region. The motivation for this model is a series of experimental studies which showed the pressure just downstream of the step to be almost constant in some upstream portion of the separated region. Previous models have ignored this constant-pressure region and agreement with experiment has not been good. Agreement with experiment is clearly superior using the constant-pressure/constant-vorticity model, though it is possible that the comparison could be improved still further by consideration of the behaviour of the shear layer after reattachment. Some discussion of such models is given

1. Introduction

In this paper we shall describe an experimental and theoretical study of the flow field of a laminar, incompressible, steady uniform stream flowing past a backward-facing step. We shall only be concerned with flows that have high Reynolds number based on step height and where the boundary-layer thickness upstream of the step is much smaller than the step height. It is frequently stated in the experimental literature that this is the simplest example of a separated flow, since the separation point is fixed and the deflection of the mainstream flow is quite gradual after separation. Figure 1 represents the generally agreed qualitative picture of the mean flow field behind such a step. The mean velocity distribution behind the step (height H) was measured by Moss & Baker (1980) and is presented in figure 2.

Near the step, the wall pressure coefficient C_p, defined by

$$C_p(x) = \frac{p(x)-p_\infty}{\frac{1}{2}\rho U_\infty^2}, \tag{1}$$

is negative, small and approximately constant. It rises gradually downstream to achieve a positive maximum near the reattachment point where the velocity at the boundary changes sign, before falling gradually to zero far downstream. This description of the pressure was confirmed in the experimental study carried out by Narayanan, Khadgi & Viswanath (1974). However, they had to make some

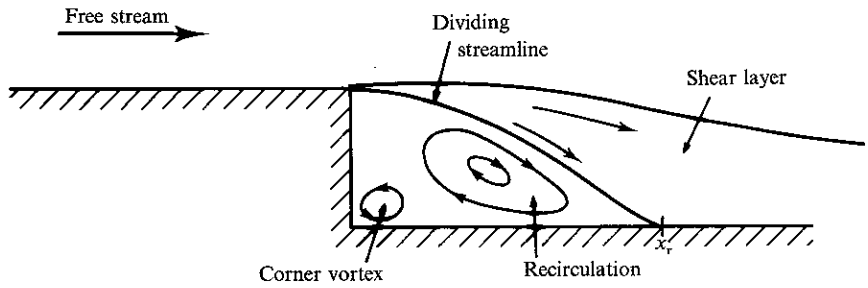

FIGURE 1 General description of the mean flow field

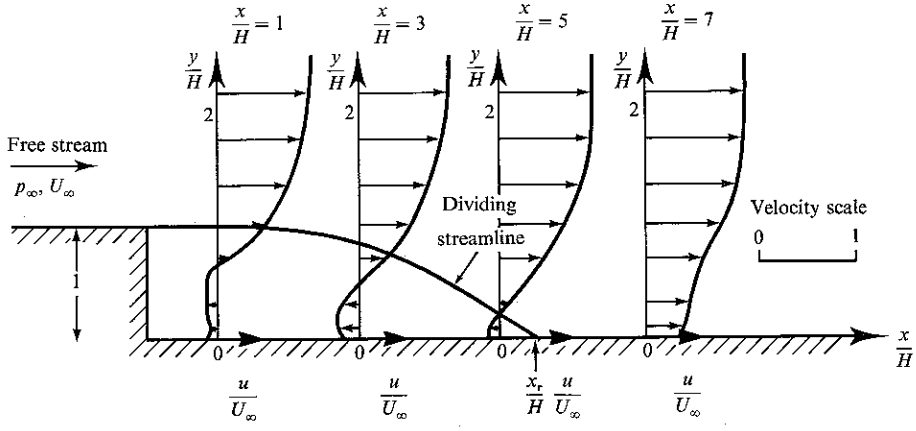

FIGURE 2 Representative velocity distributions behind a step measured by Moss & Baker (1980)

allowances for the fact that the pressure did not recover the value p_∞ of the pressure far upstream because of the increased area downstream of the step. They were able to eliminate this effect by placing area-compensating wedges on the tunnel wall opposite the step. This slightly shortened the reattachment distance for each step height, the effect being accentuated as the step height increased. It also caused the variation of the pressure coefficient with step height to be decreased and, except for the region around the step and the endpoint of the wedge at $x = 0$, the pressure distribution along the top wall of the tunnel was found to be more uniform. Figure 3 shows a selection of their results, plotting $(p-p_{\min})/(p_{\max}-p_{\min})$ against $(x-\hat{x})/H$, where $p_{\min}$ and $p_{\max}$ are respectively the minimum and maximum pressures recorded, H is the step height and $\hat{x}$ is the distance from the step to the point on the downstream wall where the pressure coefficient C_p satisfies

$$C_p(\hat{x}) = \tfrac{1}{2}(C_{p_{\max}} - C_{p_{\min}}).$$

It can be seen that the correlation collapses the results fairly successfully onto one line, and the general form of the pressure profile is as expected.

The search for similarity characteristics was also pursued by Moss & Baker (1980), who plotted the modified pressure coefficient $\bar{C}_p$ against x/x_r where x_r was the position of the reattachment point and

$$\bar{C}_p = \frac{C_p - C_{p_{\min}}}{1 - C_{p_{\min}}} = \frac{p(x) - p_{\min}}{\frac{1}{2}\rho U_\infty^2 + p_\infty - p_{\min}}. \tag{2}$$

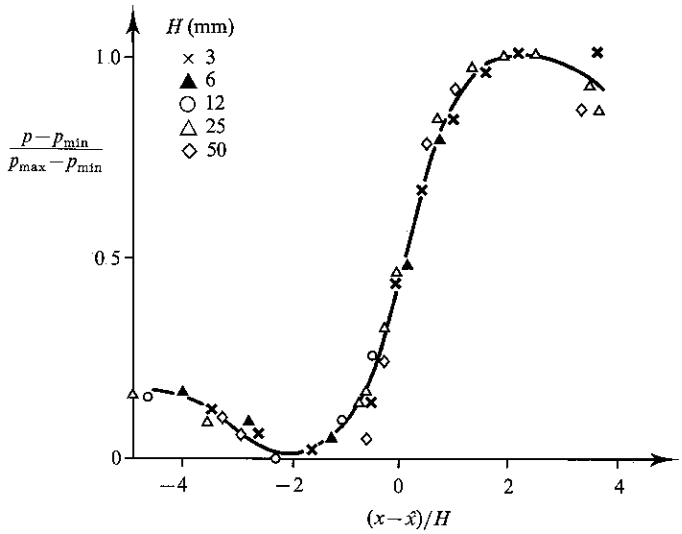

FIGURE 3. The results of Narayanan *et al* (1974) plotted in terms of $\hat{x}$, the distance from the step to the position where the average pressure coefficient is attained

They found that this correlation gave excellent agreement between four different sets of experimental data · their own and those of Narayanan *et al.* (1974), Tani, Iuchi & Komoda (1961) and Roshko & Lau (1965). The universality of these results is discussed later with reference to the experimental results of the present study

The conclusion drawn from the experimental evidence reviewed above is that separated flows behind backward-facing steps in free streams of high Reynolds number have universal features (Similar features can sometimes also be discerned in other 'thin' separated flows e.g. behind a trip on a wall (see for example Good & Joubert 1968, Ruderich & Fernholz 1986 and Eaton & Johnston 1981).) Fluid is entrained from the separated region into a turbulent shear layer which divides the separated flow from the external flow. Near its point of reattachment to the wall, the shear layer divides; part of the fluid moves upstream into the separated flow and the rest moves downstream with the external flow For steady flow, the mass of fluid entrained by the shear layer equals the mass of fluid returned to the separated flow near reattachment Turbulence measurements reveal a complex flow structure within the shear layer

At least two theoretical models have been proposed for closed recirculating regions embedded in a uniform stream when the effects of viscosity have been assumed to be confined to layers thin compared to the free-stream displacement.

One possibility is to postulate a model in the spirit of a Helmholz–Kirchhoff flow where the separated region has constant pressure, but the experimental evidence described above shows clearly that this model could only be valid over part of the separated region: indeed velocities as high as $0.4U_\infty$ have been recorded in the separated region in some cases. A further disadvantage of this model is that if p_∞ exceeds the pressure in the separated region, this region must be convex and cannot therefore reattach tangentially to the wall downstream of the step. Normal reattachment is not possible as this would require a stagnation point in the flow, so that the only solution is a flow where the dividing streamline has zero slope everywhere. This problem formally disappears in the thin-body limit except near the point of reattachment in a region which is small on the outer lengthscale. If we ignore

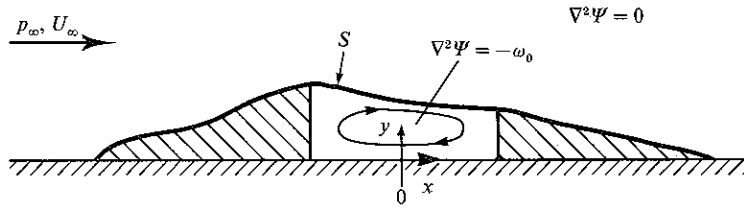

FIGURE 4 Childress flow between two obstacles.

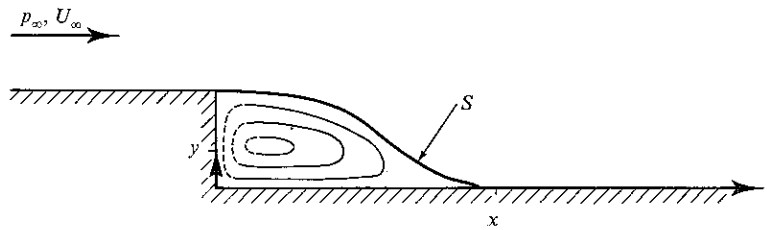

FIGURE 5 Childress' (1966) streamline pattern behind the backward-facing step

the normal reattachment difficulty the Helmholtz–Kirchhoff model may be solved uniquely when the cavity pressure and reattachment length are given; these parameters may then be related to the step height as described in §3 If these values are at variance with the experimental results then we might postulate the existence of an 'afterbody' of constant height, representing the downstream shear layer.

An alternative possibility is the Prandtl–Batchelor proposal that the vorticity is constant, not necessarily zero, in the separated region This has been studied in detail by Childress (1966) in the case of a thin region between two obstacles in an otherwise irrotational free stream (figure 4). (The Childress problem was generalized by Riley (1987). Cases where the recirculation region is not thin were considered by Sadovskii (1971) and Moore, Saffman & Tanveer (1988)) The Childress streamline pattern for the case of a backward-facing step is shown in figure 5. The broken streamlines in the figure are indicative of the fact that, since Childress assumed a thin-body approximation, his analysis is not valid near the step. It should also be noted that since the recirculating region is separated from the main flow then across the curve S there can be a jump in the Bernoulli constant h so that

$$h = \tfrac{1}{2}\rho[q_e^2 - q_i^2],$$

where q is the flow speed and the subscripts e and i represent the regions external and internal to the recirculating region respectively. The techniques employed by Childress will also be used to analyse the composite model proposed in §3, where comparison will also be made with Childress' results

Before describing the experimental details in §2, we repeat the basic assumptions which we need to make in §3 to enable analytical progress to be made. They are that the flow is steady and incompressible and that viscous effects are confined to wall boundary layers of negligible thickness, a shear layer near the dividing streamline across which entrainment is negligible and, of course, to the generation of any constant-vorticity region which may be present. We also assume that all flow deflections from the free-stream direction are small.

With these assumptions, it transpires that the dividing streamline is the easiest flow variable to predict analytically The most easily measured flow variable is the

wall pressure coefficient, but, assuming small flow deflections, these two quantities are simply related to each other through a Hilbert transform (see the Appendix).

2. The experimental measurement of pressure and velocity distributions for flow down a step

The experiments were conducted using an open loop wind tunnel to provide the flow. The dimensions of the working section were 50 cm × 50 cm, and a 30 mm step was constructed from Perspex 1.5 mm thick bolted to the wall. The flow in the tunnel was driven by an electrofan at the downstream end of the tunnel which drew air from the atmosphere via a two-dimensional bellmouth with a flow straightener and gauze at the inlet. In order to minimize boundary-layer effects, the step had a length of only 20 cm, and uniformity of the flow approaching the step was maintained by extracting air from beneath the step via a connection to a low-pressure region downstream of a resistance. The experimental arrangement is shown in figure 6. The free-stream total pressure was measured by a probe situated on the far side of the tunnel opposite the step. Static pressures on the wall upstream of the step, the step wall itself, and the wall downstream of the step were measured with respect to the static free-stream pressure using an electronic manometer. Flow velocities within the separated flow region were lower than the free-stream velocities, falling to zero at the point of flow reversal. Thus very low velocities were to be measured. It was also necessary to determine the direction of the flow. To perform both functions, a special Pitot probe was constructed which consisted of a very small tube with a small hole drilled in the side. Measurements of Pitot pressure were made with the hole pointing either upstream or downstream and the position of flow reversal was found when these two pressures were equal. This measurement gave the local static pressure which in turn allowed the static pressure and the local velocity to be found. The measurements were made with respect to the nearest wall static tapping in order to increase the accuracy. This method constitutes a simple but effective method of flow measurement in a separated region. The free-stream dynamic head $p_{t\infty}-p_\infty$ in the experiments was 38.61 mm Hg (where $p_{t\infty}$ denotes the total free-stream pressure) and the Reynolds number based on the step height was 1.9×10^5.

The results of the experiments showed that the upstream wall boundary layer separates from the corner of the step (figure 7). It forms a free shear layer bounded below by a region of recirculating flow with large mean velocities and above by external irrotational flow. The pressure coefficient maintains an approximately constant value over the first three-fifths of the separated region, then rises monotonically over the remaining distance to the reattachment point. After reattachment of the boundary of the separated flow to the wall downstream of the step, the velocity profiles indicate that the shear layer persists for long distances downstream, and with a thickness which is of the same order of magnitude as the step height. In order to test the experimental data against that collected by Narayanan *et al.* (1974), Tani *et al.* (1961), Moss & Baker (1980) and Roshko & Lau (1965), all five sets of results were plotted to reveal the variation of the coefficient $\bar{C}_p$ with x/x_r (figure 8). It can be seen that there is an excellent agreement. Although not much explanation has been given in the literature regarding the remarkable universality of this form of correlation, it seems clear that such a presentation of results must be more accurate than merely plotting the pressure coefficient C_p against x/x_r, because the expression does not explicitly contain the undisturbed static pressure p_∞. In

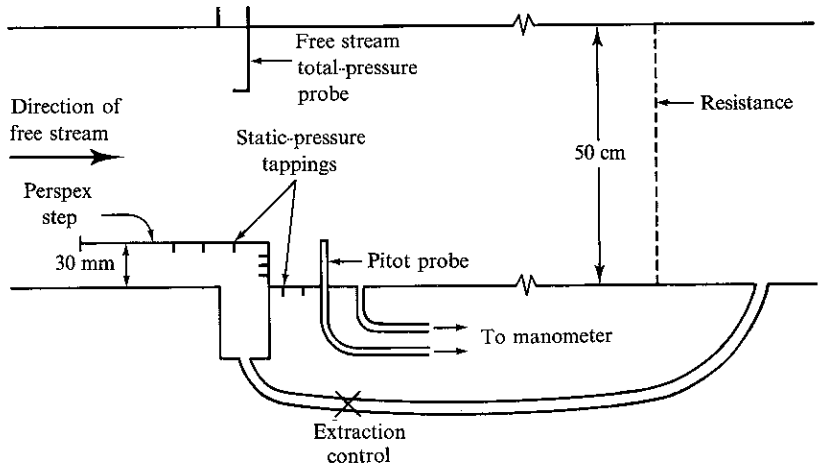

FIGURE 6. Plan view of working section of tunnel

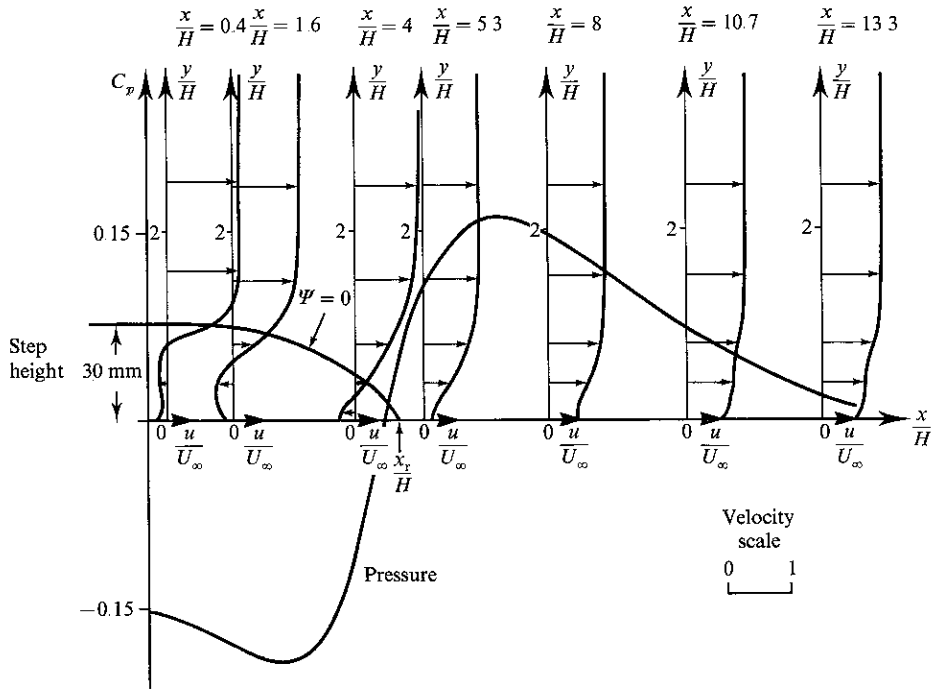

FIGURE 7. Velocity and pressure distributions for 30 mm step

experiments designed to measure the pressure distribution on the wall of a backward-facing step, the accuracy of the measurement of p_∞ is likely to be affected both by the fact that it is measured at different locations and also by whether corrections to the wind tunnel wall are made to account for blockage effects. Assuming Reynolds-number independence, $\bar{C}_p$ will be a function of non-dimensional distance from the step wall only.

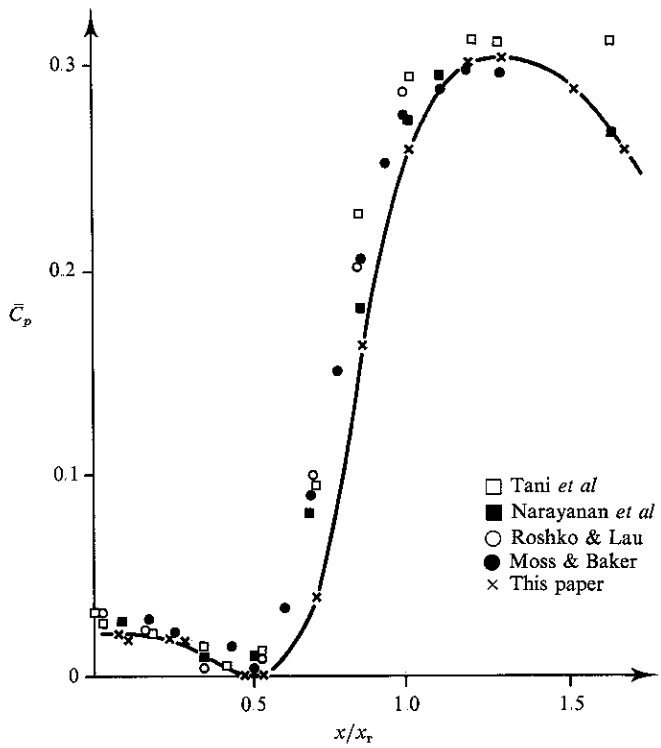

FIGURE 8 Graph of $(C_p - C_{p_{\min}})/(1 - C_{p_{\min}})$ against x/x_r for the five sets of data.

3. A composite model for flow past a backward-facing step

We now propose a model of the flow past a step in which the separated flow is represented by a closed region of fluid at constant pressure followed by a closed region of recirculating fluid (figure 9). The separated flow is again assumed to be bounded by a thin shear layer. The velocity profiles for the flow past the step indicate that the vorticity of the recirculating flow is close to constant from the end of the region of constant pressure downstream of the step to the reattachment point. Thus the present model is similar to the analysis of Childress but differs in that the separated flow is assumed to give rise to a *constant* wall pressure coefficient for a distance L downstream of the step. In practice, it is likely that the flow will contain multiple eddies near to the wall rather than just a single vortex. The present model is therefore the simplest multiple-eddy model that could be proposed. We suppose that the shear layer reattaches to the wall at a distance αL ($\alpha > 1$) downstream of the step, enclosing a constant-vorticity region of recirculating flow in $L < x < \alpha L$. Thus the coordinates of the separation and reattachment points of the shear layer are taken to be $(0, H)$ and $(\alpha L, 0)$ respectively The irrotational free-stream flow is designated region I, and the separated region is divided into region II, where the pressure is constant, and region III, where the vorticity is constant. The vorticity in the proposed model represents the vortical nature of the true flow. Although it cannot be expected to capture the full structure of the real flow, it may be interpreted as averaged vorticity.

We recall that the thickness of the separated shear layer is assumed to be an order of magnitude smaller than the thickness of the whole separated region. Moreover the

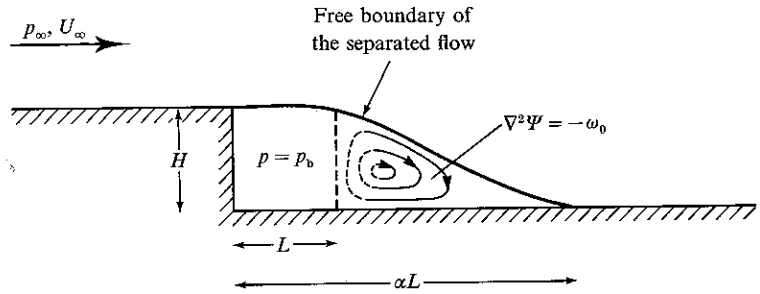

FIGURE 9 Diagram of the modelled flow field

pressure p_b in the separated region must differ from p_∞ by a small amount in order for the free-stream deflection to be small. Hence we define ϵ to be the magnitude of the constant pressure coefficient immediately downstream of separation, i.e.

$$\epsilon = \frac{p_\infty - p_b}{\frac{1}{2}\rho U_\infty^2}.$$

We could equally have defined ϵ to be the flow deflection H/L, as did Childress. However, p_b is more easily measured than L and the two definitions differ only by an $O(1)$ scaling factor λ where

$$\epsilon = \lambda \frac{H}{L}.$$

We now consistently let the thickness of the separated region be represented by

$$y = S(x;\epsilon)$$

The boundary conditions for $S(x)$ are $S(0) = H$, $S(\alpha L) = 0$, and for smooth separation at $x = 0$ and reattachment at $x = \alpha L$ without a stagnation point in the external flow we have $S'(0) = S'(\alpha L) = 0$. The values of ϵ, α and L are unknown and must be determined experimentally. The stream function in region I is represented to first order in ϵ by

$$\Psi_1(x,y;\epsilon) = U_\infty y + \frac{U_\infty}{\pi}\int_0^{\alpha L} S'(t)\tan^{-1}\frac{y}{x-t}\,\mathrm{d}t \quad (-\infty < x < \infty, \quad y \geqslant 0).$$

The boundary conditions satisfied by Ψ_1 are

$$\Psi_1 = 0 \quad \text{on} \quad y = H, \quad x < 0 \quad \text{and} \quad y = 0, \quad x > \alpha L$$
$$\Psi_1 = 0 \quad \text{on} \quad y = S(x), \quad 0 < x < \alpha L$$

The wall pressure coefficient is given by

$$C_p(x) = \frac{p(x) - p_\infty}{\frac{1}{2}\rho U_\infty^2} = -\frac{2}{\pi}\int_0^{\alpha L}\frac{S'(t)}{x-t}\,\mathrm{d}t \quad (-\infty < x < \infty)$$

and is constant in region II, $0 < x < L$.

In region III, the flow is assumed to have constant vorticity ω_0 which is to be determined; hence the stream function Ψ_3 satisfies

$$\nabla^2\Psi_3 = -\omega_0, \quad L < x < \alpha L, \quad 0 < y < S(x) \tag{3}$$

and so we take

$$\Psi_3 = 0 \quad \text{on} \quad y = 0 \quad (L < x < \alpha L) \tag{4}$$

The scalings for region II are taken to be

$$x = Lx^*, \quad y = \epsilon L y^*, \quad S(x) = \epsilon L S^*(x^*).$$

The same scalings also hold in region III where, in addition,

$$\Psi(x, y; \epsilon) = \epsilon^{\frac{3}{2}} U_\infty L \Psi^*(x^*, y^*), \quad \omega_0 = \epsilon^{-\frac{1}{2}} U_\infty \omega^*/L,$$
$$u(x, y; \epsilon) = \epsilon^{\frac{1}{2}} U_\infty u^*(x^*, y^*), \quad v(x, y; \epsilon) = \epsilon^{\frac{3}{2}} U_\infty v^*(x^*, y^*).$$

These scalings are chosen so that the pressure may be balanced across the dividing streamline and be consistent with the order of magnitude of the pressures predicted by thin-aerofoil theory. We analyse region III first; (3) and (4) become to lowest order

$$\frac{\partial^2 \Psi_3^*}{\partial y^{*2}} = -\omega^*, \quad 1 < x^* < \alpha, \quad 0 < y^* < S^*(x^*)$$

and

$$\Psi_3^* = 0 \quad \text{on} \quad y^* = 0 \quad \text{and} \quad y^* = S^*(x^*),$$

so that Ψ_3^* is given by

$$\Psi_3^*(x^*, y^*) = -\tfrac{1}{2}\omega^* y^*(y^* - S^*(x^*)), \quad 1 < x^* < \alpha, \quad 0 < y^* < S^*(x^*). \tag{5}$$

Since the pressure is continuous across the streamline dividing the external and separated flows, the jump in the Bernoulli constant across this streamline is given by

$$h = \tfrac{1}{2}\rho[(\nabla \Psi_1)^2 - (\nabla \Psi_3)^2], \quad 1 < x^* < \alpha \tag{6}$$

Substituting for Ψ_1 and Ψ_3 and expanding (6) to first order in ϵ, we find that h must therefore satisfy

$$h = \tfrac{1}{2}\rho U_\infty^2 \left[1 + \frac{2\epsilon}{\pi} \int_0^\alpha \frac{S^{*\prime}(t)}{x^* - t}\,\mathrm{d}t - \tfrac{1}{4}\epsilon\omega^{*2} S^{*2}(x^*)\right], \quad 1 < x^* < \alpha \tag{7}$$

If h^* is defined by

$$h = \rho U_\infty^2 (\tfrac{1}{2} + \epsilon h^*),$$

then it follows from (7) that

$$\frac{1}{\pi} \int_0^\alpha \frac{S^{*\prime}(t)}{x^* - t}\,\mathrm{d}t = h^* + \tfrac{1}{8}\omega^{*2} S^{*2}(x^*), \quad 1 < x^* < \alpha. \tag{8}$$

As in the Childress model described in the Introduction, where the assumption of nearly unidirectional flow breaks down near the step wall, the separated flow is fully two-dimensional near the boundary dividing the regions of constant pressure and constant vorticity defined by $x^* = 1$, $0 \leqslant y^* \leqslant S^*(1)$. However, if we assume continuity of pressure across the region near $x = L$ we must have

$$\lim_{x \downarrow L} C_p(x) = \lim_{x \uparrow L} C_p(x). \tag{9}$$

Since the experimentally observed pressure variations are small everywhere it is assumed that the left-hand side of (9) may be evaluated using the stream function Ψ_3^* defined by (5).

In region II it follows from the definition of ϵ that

$$\frac{1}{\pi} \int_0^\alpha \frac{S^{*\prime}(t)}{x^* - t}\,\mathrm{d}t = \tfrac{1}{2},$$

so that from (8) and (9) we find that

$$h^* = \tfrac{1}{2} - \tfrac{1}{8}\omega^{*2}S^{*2}(1).$$

Substituting for h^* in (8), we derive the basic equation for S^*:

$$\frac{1}{\pi}\int_0^\alpha \frac{S^{*\prime}(t)}{x^*-t}\,\mathrm{d}t = \begin{cases} \tfrac{1}{2}, & 0 < x^* < 1 \\ \tfrac{1}{2} + \tfrac{1}{8}\omega^{*2}(S^{*2}(x^*) - S^{*2}(1)), & 1 < x^* < \alpha. \end{cases}$$

By making the substitution

$$S^*(x^*) = \frac{8}{\omega^{*2}}\bar{S}(x^*)$$

the governing integro-differential equation becomes

$$\frac{1}{\pi}\int_0^\alpha \frac{\bar{S}'(t)}{x^*-t}\,\mathrm{d}t = \begin{cases} \tfrac{1}{2}A, & 0 < x^* < 1 \\ \tfrac{1}{2}A + (\bar{S}^2(x^*) - \bar{S}^2(1)), & 1 < x^* < \alpha, \end{cases} \tag{10}$$

where

$$\bar{S}(0) = A/\lambda, \quad \bar{S}(\alpha) = 0 \quad \text{and} \quad \bar{S}'(0) = \bar{S}'(\alpha) = 0, \quad \bar{S}(x^*) = O(x^{*\frac{3}{2}}) \quad \text{as} \quad x^* \downarrow 0,$$

and A satisfies

$$A = \tfrac{1}{8}\omega^{*2} = \tfrac{1}{8}\epsilon\left(\frac{\omega_0 L}{U_\infty}\right)^2$$

We may take advantage of the fact that the kernel in (10) is an odd function of x^*-t by multiplying both sides of (10) by $\bar{S}'(x^*)$ and integrating from 0 to α. The left-hand side is identically zero since the order of integration may be changed (provided $\bar{S}'(x^*) \sim o(x^{*-\frac{1}{2}})$ as $x^* \to 0$ and $\bar{S}'(x^*) \sim o((\alpha - x^*)^{-\frac{1}{2}})$ as $x^* \to \alpha$) and we arrive at the relationship

$$0 = \tfrac{2}{3}\bar{S}^3(1) - \frac{A^2}{2\lambda}$$

so that

$$\bar{S}(1) = \left(\frac{3A^2}{4\lambda}\right)^{\frac{1}{3}}. \tag{11}$$

Childress derived a similar relationship for his model by considering a global force balance. (By an extension of D'Alembert's paradox, a consideration of the kinetic energy of the fluid shows that the relative lateral displacement of the wall streamline at $x^* = \pm\infty$ must equal the horizontal force in non-dimensional terms) Such simple results are common to integral equations taking the form of (10) with the right-hand side being a function of $\bar{S}$ only and with zero-slope conditions at the ends of the range Note that (11) would still hold even without the constraint on slopes at the endpoints, but now we cannot change the order of integration as before. However, we could still appeal to the force balance argument.

Before discussing the numerical solution of (10) it is interesting to consider the dimensionality of the solutions For given values of the step height H, and the free-stream velocity U_∞, Childress was able to obtain a unique *non-dimensional* streamline height $\epsilon^{-1}S^*(x^*)$. His model therefore possessed a one-parameter family of solutions since, to obtain the fully *dimensional* solution, the length L (the analogue to (11) providing the unknown vorticity ω_0) was required. It seems plausible that the addition of the constant-pressure region might increase the dimensionality by two since p_b and α are both unknown. However p_b is the value of the pressure as $x \downarrow L$ and

as $x \uparrow L$, and in fact the dimensionality is only increased by one because we can obtain a non-trivial identity similar to (11) by multiplying (10) by $[t(\alpha-t)]^{-\frac{1}{2}}$ and integrating. This yields

$$A = -\frac{2}{\pi}\int_1^\alpha \frac{\bar{S}^2(t)-\bar{S}^2(1)}{[t(\alpha-t)]^{\frac{1}{2}}}\,\mathrm{d}t. \tag{12}$$

Equations (10) and (12) suggest that we require only one parameter, α, to obtain the non-dimensional solution for $\bar{S}(x^*)$. Since the value of λ is then known for a given H via (11), we only need the two parameters ϵ and L to finally obtain the solution in dimensional form; the present model contains two degrees of freedom. Note that once we have specified α from the experiment there is also another possibility: we might regard H as 'unknown' and use experimental data for ϵ and L to calculate a value for H. This procedure allows us to determine the 'apparent step height' which is experienced by the flow.

We may solve (10) using the procedure of Fitt, Ockendon & Jones (1985). Briefly, the idea is to avoid the processes of numerical differentiation and Hilbert transform quadrature wherever possible. The first step is to invert (10) to give

$$\bar{S}'(x^*) = \left(\frac{x^*}{\alpha-x^*}\right)^{\frac{1}{2}}\left[-\tfrac{1}{2}A + \frac{1}{\pi}\int_1^\alpha \left(\frac{\alpha-t}{t}\right)^{\frac{1}{2}}\frac{(\bar{S}^2(t)-\bar{S}^2(1))}{t-x^*}\,\mathrm{d}t\right] \quad (0 \leqslant x^* \leqslant \alpha) \tag{13}$$

where the appropriate eigensolution has been chosen to satisfy the derivative boundary conditions at the end points. Integrating (13) with respect to x^* and choosing the constant of integration to satisfy $\bar{S}(\alpha) = 0$ now yields

$$\begin{aligned}\bar{S}(x^*) = {} & \tfrac{1}{2}A\alpha\left[\frac{\pi}{2} - \sin^{-1}\left(\frac{x^*}{\alpha}\right)^{\frac{1}{2}} + \left(\frac{x^*}{\alpha}\right)^{\frac{1}{2}}\left(1-\frac{x^*}{\alpha}\right)^{\frac{1}{2}}\right] \\ & + \left[1 - \frac{2}{\pi}\sin^{-1}\left(\frac{x^*}{\alpha}\right)^{\frac{1}{2}}\right]\int_1^\alpha \left(\frac{\alpha-t}{t}\right)^{\frac{1}{2}}(\bar{S}^2(t)-\bar{S}^2(1))\,\mathrm{d}t \\ & + \frac{1}{\pi}\int_1^\alpha (\bar{S}^2(t)-\bar{S}^2(1))\log\left\{\left[\left(\frac{t}{\alpha}\right)^{\frac{1}{2}}\left(1-\frac{x^*}{\alpha}\right)^{\frac{1}{2}} + \left(\frac{x^*}{\alpha}\right)^{\frac{1}{2}}\left(1-\frac{t}{\alpha}\right)^{\frac{1}{2}}\right]^2 \Big/ \left|\frac{x^*}{\alpha}-\frac{t}{\alpha}\right|\right\}\mathrm{d}t \\ & (0 \leqslant x^* \leqslant \alpha),\end{aligned}$$

and it may be shown using (11) and (12) that the boundary condition at $x^* = 0$ is also satisfied. If the interval $(1, \alpha)$ is then discretized into sub-intervals $(t_k, t_{k+1}]\,(k = 0, \ldots, N-1)$, where $t_0 = 1$, $t_N = \alpha$, and $\bar{S}^2(t)$ is approximated as $\frac{1}{2}(\bar{S}^2(t_k)+\bar{S}^2(t_{k+1}))$ over each such interval, the scheme

$$\begin{aligned}\bar{S}_{j+1}(x^*) = {} & \alpha\left[1 - \frac{2}{\pi}\sin^{-1}\left(\frac{x^*}{\alpha}\right)^{\frac{1}{2}}\right]\sum_{k=0}^{N-1}\tfrac{1}{2}[\bar{S}_j^2(t_k)+\bar{S}_j^2(t_{k+1})-\bar{S}_j^2(1)]\{f(t_{k+1};\alpha)-f(t_k;\alpha)\} \\ & + \sum_{k=0}^{N-1}\tfrac{1}{2}[\bar{S}_j^2(t_k)+\bar{S}_j^2(t_{k+1})-\bar{S}_j^2(1)]\{g(t_{k+1}), x^*;\alpha)-g(t_k, x^*;\alpha)\},\end{aligned}$$

where

$$f(u;\alpha) = \left(\frac{u}{\alpha}\right)^{\frac{1}{2}}\left(1-\frac{u}{\alpha}\right)^{\frac{1}{2}}$$

and

$$g(u, x^*;\alpha) = \left(\frac{u}{\alpha}-\frac{x^*}{\alpha}\right)\log\left\{\left[\left(\frac{u}{\alpha}\right)^{\frac{1}{2}}\left(1-\frac{x^*}{\alpha}\right)^{\frac{1}{2}} + \left(\frac{x^*}{\alpha}\right)^{\frac{1}{2}}\left(1-\frac{u}{\alpha}\right)^{\frac{1}{2}}\right]^2 \Big/ \left|\frac{x^*}{\alpha}-\frac{u}{\alpha}\right|\right\},$$

and $j = 0, 1\ldots, 0 \leqslant x^* \leqslant \alpha$ may be applied. To ensure that the zero solution is not recovered, a further substitution

$$\bar{S}(t) = \bar{S}^2(1)\,\check{S}(t)$$

is made. The sequence of approximations $\tilde{S}_j$ converges rapidly for each α to a solution that is independent of the initial function $\tilde{S}_0$. For each specified value of α a unique $\bar{S}$ is calculated, and the general form of the solution is as expected.

4. Comparisons between theory and experiment

The experimental results described above give a value of ϵ equal to 0.18, the length of the region of constant pressure is 94.5 mm and the distance of the reattachment point of the dividing streamline to the wall, αL is measured to be 155 mm.

Figure 10 shows various theoretical and experimental pressure distributions, plotting the mean pressure coefficient $\bar{C}_p$ against x/L, the streamwise distance from the step wall, non-dimensionalized with respect to the length of the constant-pressure region. The six curves correspond to the following:

(i) The experimentally measured pressure coefficient.

(ii) Results from the Childress model, plotted so that the theoretical and experimental reattachment points coincide.

(iii) Results from the constant-pressure 'Helmholz–Kirchhoff' model. Here there is no recirculation region, so that $\alpha = 1$. The infinite pressure coefficient occurs because of the normal reattachment of the dividing streamline, as explained in the introduction.

(iv) Results from the present model with H specified, and ϵ and L measured from experiment. (In practice ϵ and L are the easiest parameters to measure from the experiment.)

(v) Results from the present model with ϵ, L and α measured from experiment, from which we can determine an 'apparent step height' as discussed further below.

(vi) Results from the present model with ϵ and L measured from experiment and the apparent step height chosen to be $\frac{3}{4}$ of the actual height H, the factor $\frac{3}{4}$ being chosen to give the best fit to the data.

The predictions from the Childress model are clearly too large, and do not exhibit the correct behaviour for large x/L. This is inevitable because $C_p(x/L) \to 0$ as $x/L \to \infty$. Thus $\bar{C}_p \to -C_{p_{\min}}/(1-C_{p_{\min}})$ as $x/L \to \infty$. Since the minimum values of the pressure coefficient are different in the Childress results from those observed experimentally, the limiting behaviours will not match. In the composite model, the small parameter in the problem is defined in terms of the properties of the constant-pressure region rather than the aspect ratio of the step height and the reattachment distance, thereby ensuring that the correct limiting behaviour is predicted and suggesting that on physical grounds this is the best way of defining ϵ. Of course, it would also be possible to present the Childress results artificially scaled to ensure that the values of $C_{p_{\min}}$ agree with experiment.

The numerical calculations which give the results (v), and which use the value of α measured from experiment determine an 'apparent step height' as mentioned previously, which is found to be between one half and one third of the actual height. In practice it is very difficult to relate the parameter α that appears in the model to any value of α that may be measured in the real flow. This suggests that the apparent step height should be considered as the key variable in the problem in preference to the quantity α that was incorporated into the model leading to the singular integro-differential equation. Indeed, when comparing the composite model with the real flow in figure 1, it is clear that the step in the model should more closely correspond to the drop from the step to the wall plus the displacement layer downstream. Owing to turbulent mixing within the shear layer the displacement thickness far

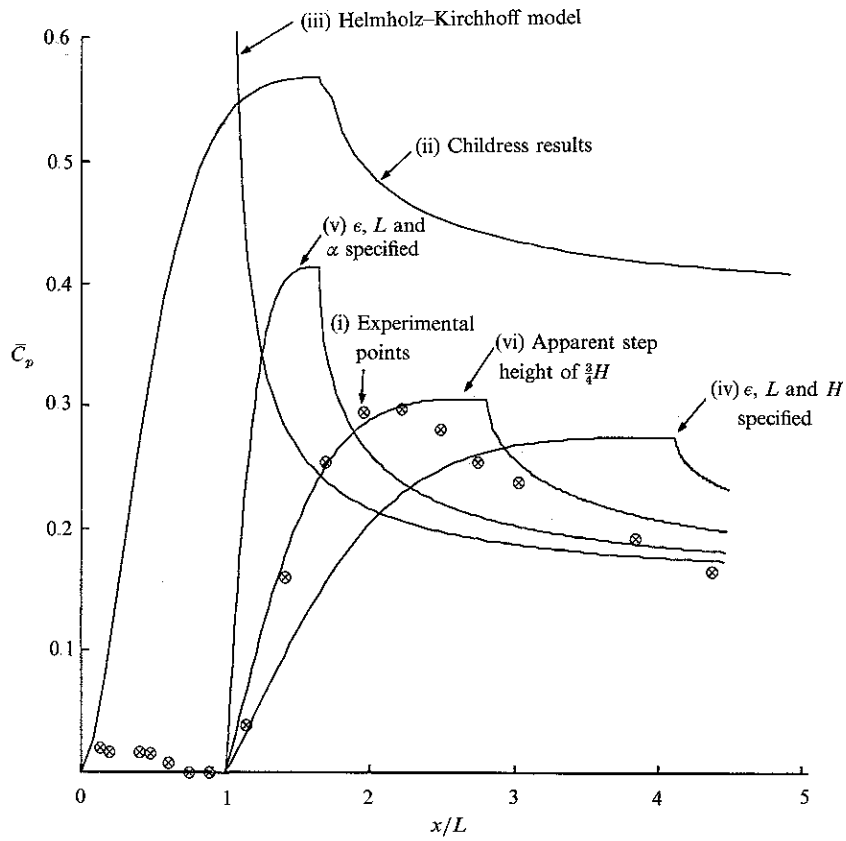

FIGURE 10 Comparison between experimental results and different theoretical models

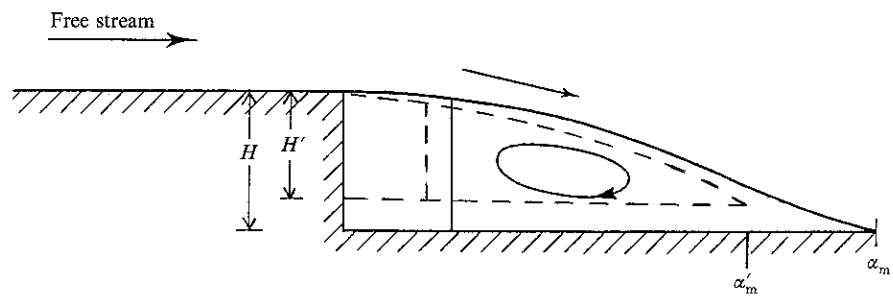

FIGURE 11 Comparison of apparent step height and reattachment length for original composite model and modified model

downstream may be a significant fraction of the step height in the real flow. Thus the step size in the model may correspond to a fraction of the real step height Figure 11 illustrates this fact, showing the relationship between the model as originally proposed and the modified model As the reattachment distance in the original model α_m increases, H increases and the vorticity ω^* decreases. The modified model that led to good agreement with experimental results corresponds to taking values of $H' < H$ and $\alpha'_m < \alpha_m$ Our strategy therefore has been to take $H' = H - H_\infty$, where the calculation in the Appendix gives $H_\infty = \frac{1}{4}H$.

In connection with the concept of apparent step height, it is of interest to calculate

the shape of the separated region experienced by the separated flow using the experimental pressure distribution. This calculation is described in the Appendix, the results showing that the separation streamline never reattaches and the apparent fall in streamline height is approximately $\frac{3}{4}$ of the step height. This is consistent with the apparent step height that gives the best fit to the experimental results.†

5. Concluding remarks

We have proposed a model for flow down a backward-facing step, employing the assumption that the separated flow region consists of a region of constant pressure followed by a region of constant vorticity. The introduction of more unknown parameters into the problem leads to a solution having one more degree of freedom than was present in the earlier model of Childress, allowing better comparisons with experiment to be made. Although there are a number of different possible ways of performing the comparison, depending on what is measured from the experimental data and what is regarded as 'known', the most successful agreement is obtained using an apparent step height which is $\frac{3}{4}$ of the true step height.

An inverse calculation may be performed on the experimental pressure-distribution data to reconstruct the shape of the dividing streamline. This suggests that under normal experimental conditions there is no actual reattachment to the wall, and instead a layer of appreciable thickness exists for all x. The calculation also leads to almost exactly the apparent step height ($\frac{3}{4}H$) that gives the best fit to the experimental data. Bearing in mind the universality of the experimental curves when plotted in the appropriate variables, it seems that fairly good agreement may be achieved by the inviscid model that has been proposed, without having to introduce complicated models of turbulence.

Clearly, to predict the flow behind steps with complete accuracy, the inclusion of viscosity is required. In spite of this, the insight which can be gained from considering inviscid models can be valuable as they give us an idea of the deficiencies and capabilities of inviscid flow theory. In addition to this, the results discussed above constitute evidence that in many separated flows there is a case for including both Helmholz–Kirchhoff and Prandtl–Batchelor regions in the flow.

The authors are grateful to the referees for their helpful comments which led to a substantial improvement in the presentation of the results in this paper. K. O'Malley acknowledges the support of the Science and Engineering Research Council.

Appendix. Calculation of the shape of the shear layer using the pressure distribution

Previously, we have used experimental observation and mathematical modelling to calculate the equation of the streamline $y = S(x)$ dividing the external flow from the wake, and, using

$$C_p(x) = \frac{p(x)-p_\infty}{\frac{1}{2}\rho U_\infty^2} = -\frac{2}{\pi}\int_{-\infty}^{\infty} \frac{S'(t)}{x-t}\,\mathrm{d}t \quad (-\infty < x < \infty) \tag{A 1}$$

† Note that it is possible to make allowances for the shear layer by proposing a constant-pressure/constant-vorticity model where the dividing streamline does not reattach to the wall downstream of the step, but instead joins with a shear layer of constant unknown height, H_2 say. We refer to this as an 'added shear layer' model. 'Reattachment' to the shear layer is still tangential, but the boundary condition is now changed. The result is a problem that can be solved numerically (details are given in O'Malley 1988) to yield a three-parameter family of solutions

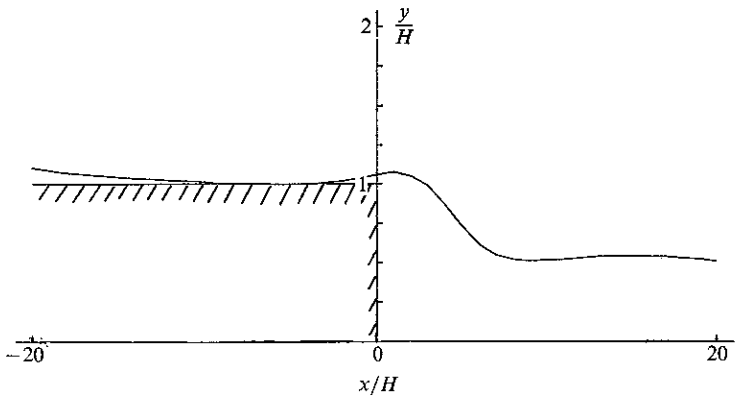

FIGURE 12 Calculated profile of $\tilde{S}(\tilde{x})$

we have calculated the resulting pressure distribution for comparison with experiment In the cases where either the step height or the length of the reattachment is measured experimentally and used in the mathematical model, agreement with the experimental results is only slightly better than for the Childress model, and the results clearly indicate that substantially better agreement would be obtained if a step height less than the true step height or a reattachment length less than the experimental reattachment length were used. The reason for this is evident · our modelling of the shear layer as a thin region over at least part of the flow is not sufficiently accurate. Indeed, the velocity profiles indicate the existence of an extensive wake region consisting of a shear layer originating near the separation point, and suggest that allowance be made for the effects of the shear-layer thickness To see how to do this, rather than using the pressure distribution as a test of our calculation, let us try a different approach and use the experimental data and (A 1) to discover the fictitious 'aerofoil' section to which the external flow actually responds Assuming that there is no appreciable transfer of fluid into the shear layer from the free stream, the thickness of the separated flow is calculated as follows First we invert (A 1) to give

$$S'(x) = \frac{1}{2\pi}\int_{-\infty}^{\infty}\left(\frac{p(t)-p_\infty}{\frac{1}{2}\rho U_\infty^2}\right)\frac{\mathrm{d}t}{x-t} \quad (-\infty < x < \infty) \tag{A 2}$$

If all lengths are non-dimensionalized with the step height H, i.e.

$$x = H\tilde{x}, \quad y = H\tilde{y}, \quad S(x) = H\tilde{S}(\tilde{x}),$$

then (A 2) becomes

$$\tilde{S}'(\tilde{x}) = \frac{1}{2\pi}\int_{-\infty}^{\infty}\left(\frac{p(u)-p_\infty}{\frac{1}{2}\rho U_\infty^2}\right)\frac{\mathrm{d}u}{\tilde{x}-u} \quad (-\infty < \tilde{x} < \infty) \tag{A 3}$$

Naturally to calculate $\tilde{S}(\tilde{x})$ from (A 3) we require data for the pressure coefficient for all real $\tilde{x}$, and experimentally this is not available. It is therefore necessary to make some assumptions about the decay of the experimental results outside the region where measurements have been taken. It should also be pointed out that to determine $\tilde{S}$ the numerical approximation to a Hilbert transform of discrete data must be integrated. This process must be carried out with some care if the result is to be both bounded at infinity and insensitive to small changes in the data. An efficient way to accomplish this is to express the known pressure data in functional

form via a linear approximation (higher-order approximations may be used but do not materially improve the accuracy) and approximate the pressure outside the experimental region using the function

$$f(\tilde{x}) = \frac{b\tilde{x}}{a^2+\tilde{x}^2}$$

with a and b suitably chosen to ensure that the integral of the pressure coefficient is zero over the real line (if this is not so then the integral of the Hilbert transform cannot possibly behave like a constant at $\tilde{x} = \pm\infty$), exhibits the correct form of decay for large $\tilde{x}$, and is continuous This functional form is especially convenient as the Hilbert transform required may now be calculated analytically. Assuming that the experimental data are given over the region $[-t_K, t_K]$, the equation of the dividing streamline may be expressed as

$$\tilde{S}(\tilde{x}) = 1+\frac{1}{2\pi}\sum_{k=-N}^{K-1}[h_k(\tilde{x},t_{k+1})-h_k(\tilde{x},t_k)]-\frac{b}{2\pi}\int_{-\infty}^{x}\frac{t}{t^2+a^2}\log\left(\frac{|t+t_K|}{|t-t_K|}\right)\mathrm{d}t$$
$$+\frac{b}{\pi}\left(\tan^{-1}\left(\frac{t_K}{a}\right)-\frac{\pi}{2}\right)\left(\tan^{-1}\left(\frac{\tilde{x}}{a}\right)+\frac{\pi}{2}\right),$$

where
$$h_k(x,t) = \tfrac{1}{2}\log|x-t|\,(A_k(t^2-x^2)+2B_k(t-k))+B_k(x-t)$$
$$-\tfrac{1}{2}A_k tx+\tfrac{1}{4}A_k(x^2-3u^2),$$
$$A_k = \frac{C_p(t_{k+1})-C_p(t_k)}{t_{k+1}-t_k}, \quad B_k = \frac{t_{k+1}C_p(t_k)-t_k C_p(t_{k+1})}{t_{k+1}-t_k}$$

Using this formula and performing the integration numerically, $\tilde{S}(\tilde{x})$ is evaluated for $\tilde{x}\in(-20.0, 20\ 0)$ and the results are plotted in figure 12 The equivalent step height may be inferred from the values of the calculated $\tilde{S}$ as $\tilde{x}\to\pm\infty$ In this case, the calculations proved to be insensitive to small changes in the data, and gave $\tilde{S}\to 0.254$ and 1 as $\tilde{x}\to\pm\infty$ respectively, which led to a total jump in $\tilde{S}$ of about 0 746. We conclude that the wake flow effectively forms a body whose thickness is of a similar order of magnitude to the step height, and that a value of about 0.75 should be used for the 'apparent step height' in order to give the best agreement with experimental results.

REFERENCES

Childress, S 1966 Solutions of Euler's equations containing finite eddies *Phys Fluids* **9**, 860–872

Eaton, J K & Johnston, J P. 1981 A review of research on subsonic turbulent flow reattachment *AIAA J.* **19**, 1093–1100.

Fitt, A D , Ockendon, J R & Jones, T. V 1985 Aerodynamics of slot-film cooling · theory and experiment. *J Fluid Mech* **160**, 15–27.

Good, M C & Joubert, P M 1968 The form drag of two-dimensional bluff plates immersed in turbulent boundary layers *J. Fluid Mech.* **31**, 547–582

Moore, D W., Saffman, P G & Tanveer, S. 1988 The calculation of some Batchelor flows · The Sadovskii vortex and rotational corner flow *Phys Fluids* **31**, 978–990

Moore, T W F 1960 Some experiments on the reattachment of a laminar boundary layer separating from a rearward-facing step on a flat plate aerofoil *J R Aero Soc* **64**, 668–672

Moss, W. D & Baker, S 1980 Recirculating flows associated with two-dimensional steps *Aero Q* **31**, 151–172.

NARAYANAN, M A B, KHADGI, Y N & VISWANATH, P R 1974 Similarities in pressure distribution in separated flow behind backward-facing steps *Aero Q* **25**, 305–312

O'MALLEY, K 1988 An experimental and theoretical investigation of slot injection and flow separation D Phil. thesis, Oxford University Department of Engineering Science

RILEY, N 1987 Inviscid separated flows of finite extent *J Engng Maths* **21**, 349–361.

ROSHKO, A & LAU, J C. 1965 Some observations on transition and reattachment of a free shear layer in incompressible flow *Proc 1965 Heat Transfer and Fluid Mechanics Institute Stanford University Press*

RUDERICH, R & FERNHOLZ, H H 1986 An experimental investigation of a turbulent shear flow with separation, reverse flow and reattachment. *J Fluid Mech* **163**, 283–322

SADOVSKII, V S 1971 Vortex regions in a potential stream with a jump of Bernoulli's constant at the boundary *Z Angew. Math Mech* **35**, 729–735

TANI, I., IUCHI, M & KOMODA, H 1961 Experimental investigation of flow separation associated with a step or a groove *Aeronautical Research Institute, University of Tokyo, Rep* 364